

Learning the kernel matrix by predictive low-rank approximations

Martin Stražar

MARTIN.STRAZAR@FRI.UNI-LJ.SI

Bioinformatics Laboratory, Faculty of Computer and Information Science

University of Ljubljana

Večna pot 113, 1000 Ljubljana, Slovenia

Tomaž Curk

TOMAZ.CURK@FRI.UNI-LJ.SI

Bioinformatics Laboratory, Faculty of Computer and Information Science

University of Ljubljana

Večna pot 113, 1000 Ljubljana, Slovenia

Abstract

Efficient and accurate low-rank approximations of multiple data sources are essential in the era of big data. The scaling of kernel-based learning algorithms to large datasets is limited by the $O(n^2)$ computation and storage complexity of the full kernel matrix, which is required by most of the recent kernel learning algorithms.

We present the `mklaren` algorithm to approximate multiple kernel matrices learn a regression model, which is entirely based on geometrical concepts. The algorithm does not require access to full kernel matrices yet it accounts for the correlations between all kernels. It uses Incomplete Cholesky decomposition, where pivot selection is based on least-angle regression in the combined, low-dimensional feature space. The algorithm has linear complexity in the number of data points and kernels. When explicit feature space induced by the kernel can be constructed, a mapping from the dual to the primal Ridge regression weights is used for model interpretation.

The `mklaren` algorithm was tested on eight standard regression datasets. It outperforms contemporary kernel matrix approximation approaches when learning with multiple kernels. It identifies relevant kernels, achieving highest explained variance than other multiple kernel learning methods for the same number of iterations. Test accuracy, equivalent to the one using full kernel matrices, was achieved with at significantly lower approximation ranks. A difference in run times of two orders of magnitude was observed when either the number of samples or kernels exceeds 3000.

1. Introduction

Kernel methods are popular in machine learning as they model relations between objects in feature spaces of arbitrary, even infinite dimension (Schölkopf and Smola, 2002). Kernels are *inner product* functions and provide means to rich representations, which is useful for learning in domains not associated to vector spaces, such as structured objects, strings or trees. Computation of inner product values for all pairs of data points to obtain the kernel matrix requires large computation and storage, which scales as $O(n^2)$ in the number of data instances. Kernel approximations are thus indispensable when learning on large datasets

and can be classified in two groups: approximations of the *kernel function* or approximations of the *kernel matrix*.

Direct approximation of the kernel function can achieve significant performance gains. A large body of work relies on approximating the frequently used Gaussian kernel, which has a rapidly decaying eigenspectrum, as proved by the Bochner’s theorem and the concept of random features (Pennington and Yu, 2015; Szabo, 2015; Rahimi and Recht, 2007). Recently, the property of matrices generated by the Gaussian kernel were further exploited to achieve sublinear complexity in the approximation rank (Yang et al., 2014; Si et al., 2014; Le et al., 2013). In another line of work, low-dimensional features can be derived for translation-invariant kernels based on their Fourier transform (Vedaldi and Zisserman, 2012). These methods currently present the most space- and time- efficient approximations, but are limited to kernels of particular functional forms.

Approximations of the kernel matrix are applicable to any symmetric positive-definite matrix even if the underlying kernel function is unknown. Such approximations, termed *data dependent*, can be obtained using the eigenvalue decomposition, by selecting a subset of data points (the Nyström method) or by using the Cholesky decomposition, which minimizes the divergence between the original matrix and its low-rank approximation (Rudi et al., 2015; Xu et al., 2015; Li et al., 2015; Gittens and Mahoney, 2013; Williams and Seeger, 2001; Fine and Scheinberg, 2001). However, these methods are unsupervised, they disregard side information, e.g., the target variables. Predictive decompositions use the target variables to obtain a supervised low-rank approximation via the Cholesky with Side Information (Bach and Jordan, 2005) or they minimize the Bregman divergence measures (Kulis et al., 2009). The effects of kernel matrix approximation has been discussed in context of sparse Gaussian processes (Quinonero Candela and Rasmussen, 2005), where the approximation leads to degenerate Gaussian process. Learning the inducing points is equivalent to learning the pivots in matrix decompositions, but can be replaced by optimizing over the whole input domain (Snelson and Ghahramani, 2006; Wilson, 2015), with necessarily continuous domain. Cao et al. (2015) relax this limitation with a hybrid approach to kernel function and inducing set optimization. All methods listed so far operate on single kernels. This presents a limitation, since the choice of optimal kernel for a given learning task is often non-trivial.

Similarly to kernel (matrix) approximation, approaches learning the optimal kernel for a given task (dependent on the data) can be classified to i) learning the kernel (covariance) function or ii) learning the kernel matrix. Learning the kernel function is possible in continuous domains, where kernel hyperparameters are optimized to match the training data (Mohsenzadeh et al., 2015; Bishop, 2006). Alternatively, kernel functions can be learned via Fourier transforms from corresponding power-spectrums (Gal and Turner, 2015; Wilson and Adams, 2013).

Multiple kernel learning (MKL) methods learn the optimal weighted sum of given kernel matrices with respect to the target variables, such as class labels (Gönen and Alpaydin, 2011). Different kernels can thus be used to model the data and their relative importance is assessed via the predictive accuracy, offering insights into the problem domain. Depending on the user-defined constraints, the resulting optimization problems are quadratic (QP) or semidefinite programs (SDP), assuming the complete knowledge of the kernel matrices. Cortes et al. (2012) solve a QP on centered kernel matrices, which corresponds to centering the data in the original input space. Low-rank approximations have been used for MKL, e.g.,

by performing Gram-Schmidt orthogonalization and subsequently MKL (Kandola et al., 2002). In a recent study, the combined kernel matrix is learned via efficient generalized Forward-backward algorithm, however assuming that low-rank approximations are available beforehand (Rakotomamonjy and Chanda, 2014). Gönen et al. develop a Bayesian treatment for joint dimensionality reduction and classification, solved via gradient descent (Gönen and Alpaydin, 2010) or variational approximation (Kaski and Gonen, 2014), while assuming access to full kernel matrices and not exploiting their symmetric structure.

In this work, we propose a joint treatment of low-rank kernel approximations and MKL. We assume an input of: i) a set of objects with corresponding continuous target variables and a ii) set of kernels that define inner products on the same objects. We designed `mklaren`, a greedy algorithm that couples Incomplete Cholesky Decomposition and Least-angle regression to learn a low-rank approximation of the combined kernel matrix. Our innovative approach to pivot column selection is closely associated to the selection of feature vectors in least-angle regression (LAR) (Efron and Hastie, 2004). At each step, the method keeps a current estimate of the regression model within the span of the current approximation. In comparison to existing methods, it has the following two advantages. First, the method is aware of multiple kernel functions. In each step, the next pivot column to be added is chosen greedily from all remaining pivot columns from all kernels. Kernels that give more information about the current residual are thus more likely to be selected. In contrast to methods that assume access to the complete kernel matrices, the importance of a kernel is estimated at the time of its approximation. Also, this is different from performing the decomposition for each kernel k_q independently and subsequently determining kernels weights. Second, the criterion only considers the gain with respect to the current regression residual; the notion of kernel matrix approximation error is completely abolished. Even though accurate approximation is proportional to the similarity of the model using the full kernel matrix (Cortes et al., 2010), it was recently shown that i) the expected generalization error is related to maximal marginal degrees of freedom rather than the approximation error and ii) empirically, low-rank approximation can lead to a regularization-like effect (Bach, 2012). Nevertheless, the residual approximation error is guaranteed to monotonically decrease by definition of Cholesky decompositions.

When explicit feature space representation is available for kernels, the relation between primal and dual regression weights is used for model interpretation. In contrast to MKL algorithms, which rely on convex optimization or Bayesian methods, our approach relies on geometrical principles solely, leading to a straightforward algorithm with low computational complexity in the number of data points and kernels.

A common assumption when applying matrix approximation or MKL is that the resulting decomposition can only be applied in *transductive learning* (Zhang et al., 2012; Lanckriet and Cristianini, 2004), i.e., the test data samples are included in the model training phase. We apply the lemma on the uniqueness of the low-rank approximation for a fixed active set to relate the Incomplete Cholesky decomposition and the Nyström method. With this we circumvent the limitation to the transductive setting, infer low-rank representation of arbitrary test data point, enabling out-of-sample prediction.

The predictive performance, run times and model interpretation were evaluated empirically on multiple benchmark regression datasets. The provided implementation of `mklaren` compared favorably against related low-rank kernel matrix approximation and state-of-the-

art MKL approaches. Additionally, we isolate the effect of low-rank approximation and compare the method with full kernel matrix MKL methods on a very large set of rank-one kernels.

The article is structured as follows. The `mklearn` algorithm with pivot column updates with the LAR-based selection criterion is presented in Section 2. Auxilliary results regarding out-of-sample prediction, model interpretation and computational complexity analysis are given in Section 3. Experimental evaluation is presented in Section 4. Description of the Least-angle regression method is given in the Appendix. The algorithm implementation and code to reproduce the presented experiments is available at <https://github.com/mstrazar/mklearn>.

2. Multiple kernel learning with least-angle regression

Let $\{\mathbf{x}_1, \mathbf{x}_2, \dots, \mathbf{x}_n\}$ be a set of points in a Hilbert space \mathcal{X} of arbitrary dimension, associated with targets $\mathbf{y} \in \mathbb{R}^n$. Let the Hilbert spaces $\mathcal{X}_1, \mathcal{X}_2, \dots, \mathcal{X}_p$ be isomorphic to \mathcal{X} and endowed with respective inner product (kernel) functions k_1, k_2, \dots, k_p . The kernels k_q are positive definite and map from $\mathcal{X}_q \times \mathcal{X}_q$ to \mathbb{R} . Hence, a data point $\mathbf{x}_i \in \mathcal{X}_q$ can be represented in multiple inner product spaces, which can be related to different data views or representations. Evaluating k_q for each pair of \mathbf{x}_i determines a kernel matrix $\mathbf{K}_q \in \mathbb{R}^{n \times n}$. The goal of a predictive (supervised) approximation algorithm is to learn the corresponding low-rank approximations $\mathbf{G}_1, \mathbf{G}_2, \dots, \mathbf{G}_p$, where $\mathbf{G}_q \in \mathbb{R}^{n \times j_q}$, $K = \sum_q j_q < n$, using additional information on the targets. In the context of regression, the regression line $\boldsymbol{\mu} \in \mathbb{R}^n$ is learned simultaneously with the approximations, as their construction depends on the residual vector $\mathbf{r} = \mathbf{y} - \boldsymbol{\mu}$.

The `mklearn` algorithm simultaneously learns low-rank approximations of kernel matrices \mathbf{K}_q associated to each kernel function k_q and the regression line $\boldsymbol{\mu}$. It uses Incomplete Cholesky Decomposition (ICD) to iteratively construct each \mathbf{G}_q . At each iteration, a kernel k_q and a pivot column $i \in 1, 2, \dots, n$ are chosen using a heuristic that evaluates the explained information on the residual \mathbf{r} for each potential new column of \mathbf{G}_q . This is achieved by using least-angle regression in the space spanned by the previously selected (normalized and centered) pivot columns of all \mathbf{G}_q .

The high-level pseudo code of the `mklearn` algorithm is shown in Algorithm 1, and its steps are described in detail in the following subsections.

2.1 Simultaneous Incomplete Cholesky decompositions

We start with the description of Incomplete Cholesky Decomposition (ICD) of a single kernel matrix, and later extend it to simultaneous decomposition of multiple kernels. A kernel matrix \mathbf{K} is approximated with a Cholesky factor \mathbf{G} . The ICD is a family of methods that produce a finite sequence of matrices $\mathbf{G}^{(1)}, \mathbf{G}^{(2)}, \dots, \mathbf{G}^{(j)}$, such that

$$\mathbf{G}^{(j)} \mathbf{G}^{(j)T} \rightarrow \mathbf{K} \text{ as } j \rightarrow n. \quad (1)$$

Initially, \mathbf{G} is initialized to $\mathbf{0}$. A diagonal vector representing the lower-bound on the approximation gain is initialized as $\mathbf{d} = \text{diag}(\mathbf{K})$. The active set $\mathcal{A} = \emptyset$, keeping track of selected pivot columns. At iteration j , a pivot i is selected from the remaining set $\mathcal{J} = \{1, 2, \dots, n\} \setminus \mathcal{A}$ and its pivot column $\mathbf{G}(:, j) \leftarrow \mathbf{g}_i$ is computed as follows:

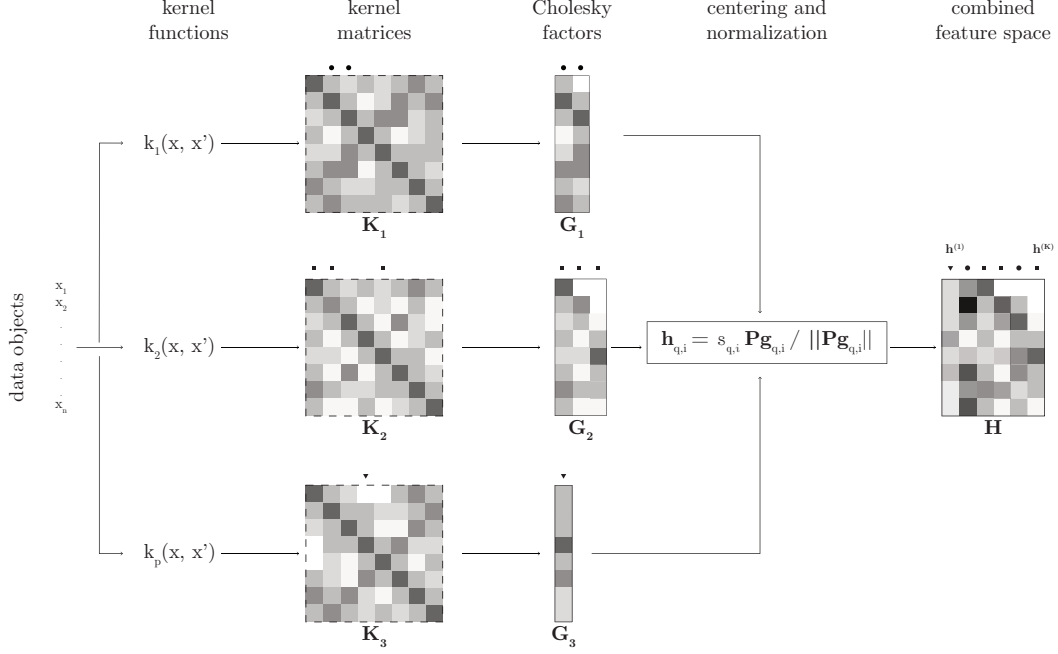


Figure 1: Overview of variables included in the hypothetical model using three kernels, $q \in \{1, 2, 3\}$. Kernel matrices in dashed values are never computed explicitly. The markers *circle*, *rectangle* and *triangle* represent the selected pivot columns for kernels 1, 2 and 3 respectively.

$$\begin{aligned} \mathbf{G}(i, j) &= \sqrt{\mathbf{d}(i)} \\ \mathbf{G}(\mathcal{J}, j) &= \frac{1}{\mathbf{G}(i, j)} \left(\mathbf{K}(\mathcal{J}, i) - \sum_{l=1}^{j-1} \mathbf{G}(\mathcal{J}, l) \mathbf{G}(i, l) \right) \end{aligned} \quad (2)$$

Importantly, only the information on one column of \mathbf{K} is required at each iteration and $\mathbf{G}\mathbf{G}^T$ need never be computed explicitly. The selected pivot is added to the active set, the counter j and the diagonal vector are updated:

$$\begin{aligned} \mathbf{d} &\leftarrow \mathbf{d} - \mathbf{g}_j^2 \\ \mathcal{A} &\leftarrow \mathcal{A} \cup \{i\} \\ j &\leftarrow j + 1 \end{aligned} \quad (3)$$

In the case of multiple, p kernels, each kernel function k_q , $q \in 1, 2, \dots, p$ determines a corresponding \mathbf{K}_q , which is approximated with Cholesky factors \mathbf{G}_q . An example scenario is depicted on Fig. 1.

The set of all Cholesky factors \mathbf{G}_q is used to construct a *combined feature matrix* to be used for least-angle regression, as follows. At any point, assume the existence of the residual

vector \mathbf{r} , to be constructed in Section 2.2. For each selected pivot column $\mathbf{g}_{q,i}$ in kernel q define the following transformation.

$$\mathbf{h}_{q,i} \leftarrow s_{q,i} \mathbf{P} \mathbf{g}_{q,i} / \|\mathbf{P} \mathbf{g}_{q,i}\| \quad (4)$$

where the operator \mathbf{P} is the centering projection $\mathbf{P} = (\mathbf{I} - \frac{\mathbf{1}\mathbf{1}^T}{n})$ and $s_{q,i}$ is the sign of the correlation $(\mathbf{P} \mathbf{g}_{q,i})^T \mathbf{r}$. Each $\mathbf{h}_{q,i}$ is normalized and makes an angle at most 90 degrees with the residual \mathbf{r} . The set of columns $\mathbf{h}_{q,i}$ span the *combined feature space*, equivalent to any matrix $\mathbf{H} \in \mathbb{R}^{n \times \sum_q j_q}$ containing this same set of columns (in any order).

$$\text{span}(\mathbf{H}) = \text{span}(\{\mathbf{h}_{1,1}, \mathbf{h}_{1,2}, \dots, \mathbf{h}_{1,j_1}, \mathbf{h}_{2,1}, \dots, \mathbf{h}_{2,j_2}, \mathbf{h}_{p,1}, \dots, \mathbf{h}_{p,j_p}\}) \quad (5)$$

The Fig. 1 shows one such matrix. Note that applying the operator \mathbf{P} is equivalent to centering the positive semidefinite matrix $\mathbf{H}\mathbf{H}^T$, which represents the *combined kernel*.

Least-angle regression is used to iteratively select the next pivot column and thus determine the order of columns in \mathbf{H} while simultaneously updating the regression line. The next kernel q and pivot j are selected from all remaining sets \mathcal{J}_q , based on the current residual \mathbf{r} . The corresponding pivot column $\mathbf{g}_{q,i}$ is computed using the Cholesky step in Eq. 2 and added to \mathbf{G}_q . At any iteration, each \mathbf{G}_q may contain a different number of columns j_q as their selection depends on the relevance for explaining the residual.

2.2 Pivot selection based on Least-angle regression

Least-angle regression (LAR) is an *active set method*, for feature subset selection in linear regression (see Appendix and Efron and Hastie (2004) for thorough description). Here, we propose an idea based on the LAR column selection to determine the next pivot column to be added to any of the \mathbf{G}_q and consequently to combined feature matrix \mathbf{H} .

The original LAR method assumes availability of all variables representing the covariates (column vectors) in the sample data matrix. In our case, however, this matrix is \mathbf{H} and is constructed iteratively. The adaptation of the LAR-based column selection is non-trivial, since the exact values of the new columns $\mathbf{g}_{q,i}$ and $\mathbf{h}_{q,i}$ are unknown at selection time.

This section describes a method to construct \mathbf{H} given the columns $\mathbf{h}_{q,i}$ and learn $\boldsymbol{\mu} \in \text{span}(\mathbf{H})$. In favor of clarity we assume (only in this section) that values of all $\mathbf{h}_{q,i}$ are known and describe the ordering of $\mathbf{h}_{q,i}$ in \mathbf{H} . The problem of unknown candidate pivot column values is postponed to Section 2.3.

The matrix \mathbf{H} is initialized to $\mathbf{0}$. The regression line $\boldsymbol{\mu}$ and the residual \mathbf{r} are initialized

$$\boldsymbol{\mu} = \mathbf{0} \text{ and } \mathbf{r} = \mathbf{y}, \text{ assuming w.l.g. } \mathbf{1}^T \mathbf{y} = 0. \quad (6)$$

By construction, $\|\mathbf{h}_{q,i}\| = 1$ and $\mathbf{1}^T \mathbf{h}_{q,i} = 0$ for all q, i . The $\mathbf{h}_{q,i}$ will be added to \mathbf{H} in a defined ordering

$$\mathbf{H}(:, l) \leftarrow \mathbf{h}_{q,i} = \mathbf{h}^{(l)} \text{ for } l = 1, 2, \dots, \sum_q j_q \quad (7)$$

where a unique kernel, pivot pair q, i is selected for each position l . The ordering depends on the correlation with the residual $c_l = \mathbf{r}^T \mathbf{h}^{(l)}$. Therefore, the Cholesky factors \mathbf{G}_q containing pivot columns with more information on the current residual are selected preferably.

The column selection procedure is depicted in Fig. 2a and is defined as follows. At iteration $l = 1$, the first vector $\mathbf{h}^{(1)}$ is chosen to maximize correlation $\mathbf{h}^{(1)} = \max_{m=1 \dots \sum_q j_q} c_m = \mathbf{r}^T \mathbf{h}^{(m)}$. This $\mathbf{h}^{(1)}$ is added to $\mathbf{H}(:, 1) = \mathbf{h}^{(1)}$.

At each iteration l , \mathbf{H} contains l columns $\mathbf{h}^{(1)}, \mathbf{h}^{(2)}, \dots, \mathbf{h}^{(l)}$. By elementary linear algebra, there exist the *bisector* \mathbf{u} , having $\|\mathbf{u}\| = 1$ and making equal angles, less than 90 degrees, between the residual \mathbf{r} and vectors currently in \mathbf{H} . Updating the regression line $\boldsymbol{\mu}$ along direction \mathbf{u} and the residual r

$$\boldsymbol{\mu}^{\text{new}} = \boldsymbol{\mu} + \gamma \mathbf{u} \quad \mathbf{r}^{\text{new}} = \mathbf{r} - \gamma \mathbf{u} \quad (8)$$

causes the correlations $c_l = \mathbf{r}^T \mathbf{h}^{(l)}$ to change equally for all $\mathbf{h}^{(l)}$ in \mathbf{H} , for an arbitrary step size $\gamma \in \mathbb{R}$. The value γ is set such that some new column $\mathbf{h}^{(l+1)}$ not in \mathbf{H} will have the same correlation to $\mathbf{r}^{(\text{new})}$ as all the columns already in \mathbf{H} :

$$\angle(\mathbf{r}^{\text{new}}, \mathbf{h}^{(1)}) = \dots = \angle(\mathbf{r}^{\text{new}}, \mathbf{h}^{(l)}) = \angle(\mathbf{r}^{\text{new}}, \mathbf{h}^{(l+1)}) \quad (9)$$

The step size γ and $\mathbf{h}^{(l+1)}$ are selected as follows. Define the following quantities

$$C = \max_{\{l | \mathbf{h}^{(l)} \in \mathbf{H}\}} c_l \quad A = (\mathbf{1}^T \mathbf{H} \mathbf{1})^{-1/2}. \quad (10)$$

Then,

$$\begin{aligned} \gamma &= \min^+_{\{m | \mathbf{h}^{(m)} \notin \mathbf{H}\}} \left\{ \frac{C - c_m}{A - a_m}, \frac{C + c_m}{A + a_m} \right\}, \text{ where} \\ c_m &= \mathbf{r}^T \mathbf{h}^{(m)} \\ a_m &= \mathbf{u}^T \mathbf{h}^{(m)}. \end{aligned} \quad (11)$$

Here, \min^+ is the minimum over positive arguments for each choice of m . The selected column vector $\mathbf{h}^{(m)}$ is the minimizer of Eq. 11 and is inserted at the $l + 1$ -th position in \mathbf{H} , $\mathbf{H}(:, l + 1) = \mathbf{h}^{(m)}$. For the last column vector (as there are no further column vectors to choose from) the step size simplifies to $\gamma = C/A$, yielding the ordinary least-squares solution for \mathbf{H} and \mathbf{y} .

The mentioned problem in our case is that the exact values of all potential pivot columns $\mathbf{g}_{q,i}$ not in \mathbf{G}_q and its corresponding $\mathbf{h}_{q,i}$ are unknown. Explicit calculation of all columns using the Cholesky step in Eq. 2 would yield quadratic computational complexity, as their values are dependent on all previously selected pivots. The issue is addressed by using approximations $\hat{\mathbf{g}}_{q,i}$ and $\hat{\mathbf{h}}_{q,i}$ that are less expensive to compute, as described in the following section.

2.3 Look-ahead decompositions

The selection of a new column vector $\mathbf{h}^{(m)}$ to be added to the combined feature matrix \mathbf{H} and its corresponding $\mathbf{h}_{g,i}$, $\mathbf{g}_{q,i}$ is based only on the values a_m , c_m in Eq. 11. Instead of explicitly calculating each candidate $\mathbf{g}_{q,i}$ for all q, i at each iteration, we use an approximate column vector $\hat{\mathbf{g}}_{q,i}$. The approach uses a similar idea to look-ahead (information) columns in (Cao et al., 2015; Bach and Jordan, 2005).

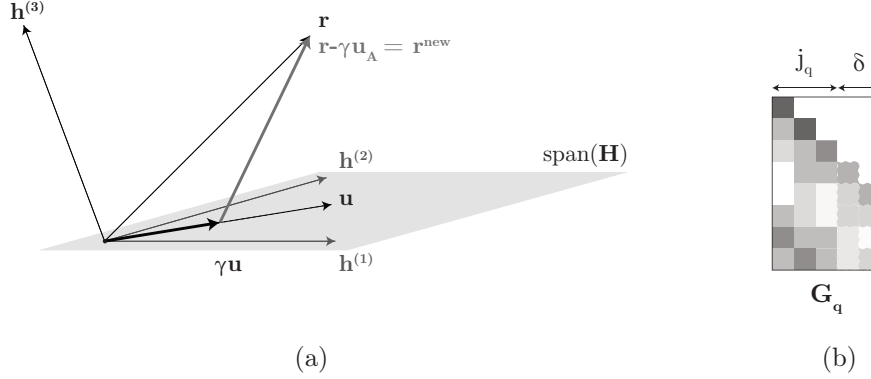


Figure 2: a) Updating the regression line within the combined feature matrix \mathbf{H} containing two vectors $\mathbf{h}^{(1)}$ and $\mathbf{h}^{(2)}$. The residual is $\mathbf{r} = \mathbf{y} - \boldsymbol{\mu}$, where $\boldsymbol{\mu} \in \text{span}(\mathbf{h}^{(1)})$ and $\angle(\mathbf{r}, \mathbf{h}_2) = \angle(\mathbf{r}, \mathbf{h}_1)$. The new residual \mathbf{r}^{new} upon selection of $\mathbf{h}^{(2)}$ is obtained by adding $\gamma\mathbf{u}$ to $\boldsymbol{\mu}$ and updating \mathbf{r} accordingly. The step size γ is increased until some new vector $\mathbf{h}^{(3)}$ will have the same correlation (angle) with \mathbf{r}^{new} as both $\mathbf{h}^{(1)}$ and $\mathbf{h}^{(2)}$, i.e., $\angle(\mathbf{r}^{new}, \mathbf{h}_3) = \angle(\mathbf{r}^{new}, \mathbf{h}_2) = \angle(\mathbf{r}^{new}, \mathbf{h}_1)$. b) Schematic representation of selected j_q pivot columns and δ look-ahead columns.

Consider the kernel matrix \mathbf{K}_q , its current Cholesky factor \mathbf{G}_q and active set \mathcal{A}_q . By definition of ICD in Eq. 2, the values of a candidate pivot column $\mathbf{g}_{q,i}$ at step j and pivot $i \notin \mathcal{A}_q$ are:

$$\mathbf{g}_{q,i} = \frac{(\mathbf{K}_q - \sum_{l=1}^{j_q} \mathbf{G}_q(:, l) \mathbf{G}_q(:, l)^T)(:, i)}{\sqrt{\mathbf{d}_q(i)}} \quad (12)$$

The main computation cost in the above definition is the computation of a rank- n kernel matrix \mathbf{K}_q for each m . Instead, δ look-ahead columns are used to get a *look-ahead approximation* $\mathbf{L}_q = \mathbf{G}_q(:, j_q + \delta) \mathbf{G}_q(:, j_q + \delta)^T$ (Fig. 2b). This defines approximate values $\hat{\mathbf{g}}_{q,i}$:

$$\begin{aligned} \hat{\mathbf{g}}_{q,i} &= \frac{(\mathbf{L}_q - \sum_{l=1}^{j_q-1} \mathbf{G}_q(:, l) \mathbf{G}_q(:, l)^T)(:, i)}{\sqrt{\mathbf{d}_q(i)}} \\ &= \frac{\mathbf{G}_q(:, j_q+1:j_q+\delta) \mathbf{G}_q^T(j_q+1:j_q+\delta, i)}{\sqrt{\mathbf{d}_q(i)}} \end{aligned} \quad (13)$$

Given $\hat{\mathbf{g}}_{q,i}$ and consequently $\hat{\mathbf{h}}_{q,i}$, consider the computation of $\hat{c}_{q,i}$:

$$\hat{c}_{q,i} = \mathbf{r}^T \hat{\mathbf{h}}_{q,i} = \frac{|(\mathbf{P} \hat{\mathbf{g}}_{q,i})^T \mathbf{r}|}{\|\mathbf{P} \hat{\mathbf{g}}_{q,i}\|} \quad (14)$$

Inserting $\hat{\mathbf{g}}_{q,i}$ as in Eq. 13, the denominator $1/\sqrt{\mathbf{d}_q(i)}$ cancels out. The norm $\|\mathbf{P} \hat{\mathbf{g}}_{q,i}\|$ can be computed as:

$$\begin{aligned} \|\mathbf{P} \hat{\mathbf{g}}_{q,i}\|^2 &= \left(\mathbf{P} \mathbf{G}_q(:, j_q+1:j_q+\delta) \mathbf{G}_q^T(j_q+1:j_q+\delta, i) \right)^T \left(\mathbf{P} \mathbf{G}_q(:, j_q+1:j_q+\delta) \mathbf{G}_q^T(j_q+1:j_q+\delta, i) \right) \\ &= \mathbf{G}_q(i, :) \left(\mathbf{G}_q^T \mathbf{G}_q(j_q+1:j_q+\delta, j_q+1:j_q+\delta) - \mathbf{G}_q^T \mathbf{1} \mathbf{1}^T \mathbf{G}_q(j_q+1:j_q+\delta, j_q+1:j_q+\delta) \right) \mathbf{G}_q(i, :)^T \end{aligned} \quad (15)$$

Similarly, dot product with the residual is computed as:

$$\begin{aligned} (\mathbf{P} \hat{\mathbf{g}}_{q,i})^T \mathbf{r} &= \mathbf{r}^T \left(\mathbf{P} \mathbf{G}_q(:, j_q+1:j_q+\delta) \mathbf{G}_q^T(j_q+1:j_q+\delta, i) \right)^T = \\ &= \left(\mathbf{r}^T \mathbf{G}_q(:, j_q+1:j_q+\delta) - \mathbf{r}^T \mathbf{1} \mathbf{1}^T \mathbf{G}_q(:, j_q+1:j_q+\delta) \right) \mathbf{G}_q(j_q+1:j_q+\delta, i) \end{aligned} \quad (16)$$

Computation of $\hat{a}_{q,i}$ is analogous. Correctly ordering the order of computation yields the computational complexity $O(\delta^2)$ per column. Note that matrices $\mathbf{G}_q^T \mathbf{G}_q$, $\mathbf{G}_q^T \mathbf{1} \mathbf{1}^T \mathbf{G}_q$, $\mathbf{r}^T \mathbf{G}_q$, $\mathbf{r}^T \mathbf{1} \mathbf{1}^T \mathbf{G}_q$ are the same for all columns (independent of i) and need to be computed only once per iteration.

The values $\hat{a}_{q,i}$ and $\hat{c}_{q,i}$ can be computed efficiently for all kernel matrices and enable the selection of next kernel, pivot column pair q, i to be added to \mathbf{G}_q and consequently \mathbf{H} . After selecting q, i a Cholesky step is performed (Eq. 2) to compute the exact $\mathbf{g}_{q,i}$ and

$$\mathbf{G}_q(:, j) \leftarrow \mathbf{g}_{q,i} \quad (17)$$

The computation of a new column renders the look-ahead columns in \mathbf{G}_q at indices $j_q+1:j_q+\delta$ invalid. After applying Eq. 17, all columns at indices $j_q+1:j_q+\delta$ are recomputed using standard Cholesky step with pivot selection based on current maximal value in \mathbf{d}_q at a cost $O(n\delta^2)$.

The exact values of $\mathbf{g}_{q,i}$ and $\mathbf{h}_{q,i}$ determine $\mathbf{h}^{(m)}$ to be added to \mathbf{H} and enables the correct computation of a_m , c_m and step size γ in Eq. 11. The regression line $\boldsymbol{\mu}$ and the residual \mathbf{r} can be correctly updated according to Eq. 8.

2.4 The mklaren algorithm

The steps described in previous sections complete the **mklaren** algorithm. Given a sample of n data objects with a targets \mathbf{y} and p kernel functions, the user specifies three additional parameters: the maximum rank K of combined feature matrix, number of look-ahead columns δ and L_2 regularization parameter λ (constraining $\boldsymbol{\mu}$, discussed in Section 3.4).

The variables related to regression line ($\boldsymbol{\mu}$, residual \mathbf{r} and bisector \mathbf{u}) and individual decompositions \mathbf{G}_q (active sets \mathcal{A} , column counters j_q) are initialized in lines 1-6. Each \mathbf{G}_p

is initialized using standard ICD with δ look-ahead columns, as described in Section 2.3 (line 7).

The main loop is executed for K iterations, until the sum of selected pivot columns equals $\sum_q j_q = K$, where at each iteration a kernel k_q and a pivot column i , $i \notin \mathcal{A}_q$ are selected and added to \mathbf{G}_q and consequently the combined feature matrix \mathbf{H} . For each kernel k_q and each pivot $i \notin \mathcal{A}_q$, $\hat{a}_{q,i}$ and $\hat{c}_{q,i}$ are computed. Based on these approximated values, the kernel k_q and pivot i are selected. Given the optimal k_q and pivot i , the pivot column $\mathbf{g}_{q,i}$ and $\mathbf{h}_{q,i}$ are computed. The new pivot column $\mathbf{g}_{q,i}$ is added to $\mathbf{G}_q(:, j_q)$, j_q is incremented and the δ columns at $\mathbf{G}_q(:, j_q+1:j_q+\delta)$ are recomputed using standard ICD (lines 9-15).

Having computed the exact $\mathbf{g}_{q,i}$, the true values $a_{q,i}$ and $c_{q,i}$ can be computed and the regression line $\boldsymbol{\mu}$ and the residual are updated (lines 16-20).

The regression coefficients $\boldsymbol{\beta}$ solving $\mathbf{H}\boldsymbol{\beta} = \boldsymbol{\mu}$, required for out-of-sample prediction, can be obtained by constructing \mathbf{H} and solving a linear system discussed in Section 3.1 (line 21).

3. Auxiliary theoretical results

This section presents auxiliary theoretical results required for out-of-sample prediction (Sections 3.1-3.2), model interpretation using the relation between primal and dual regression coefficients (Section 3.3), L_2 regularization (Section 3.4), and computational complexity (Section 3.5).

3.1 Computing the regression coefficients

The regression coefficients $\boldsymbol{\beta} \in \mathbb{R}^K$ are computed from the regression line $\boldsymbol{\mu}$ and the combined feature space \mathbf{H} as defined in Eq. 5. using the relation

$$\mathbf{H}\boldsymbol{\beta} = \boldsymbol{\mu} \implies \boldsymbol{\beta} = (\mathbf{R}^T \mathbf{R})^{-1} \mathbf{Q}^T \boldsymbol{\mu}, \quad (18)$$

where $\mathbf{H} = \mathbf{Q}\mathbf{R}$ is the thin QR decomposition Golub and Van Loan (2012).

3.2 Out-of-sample prediction

Inference of Cholesky factors corresponding to test (unseen) samples is possible without explicitly repeating the Cholesky steps. The coefficients $\boldsymbol{\beta}$ are then used to predict the responses for new samples. To simplify notation, we show the approach for one kernel matrix and its corresponding Cholesky factors, while the computation for multiple kernels is analogous.

Nyström approximation. Let $\mathcal{A} = \{i_1, i_2, \dots, i_j\}$ be an arbitrary active set of pivot indices. The Nyström approximation (Williams and Seeger, 2001) of the kernel matrix \mathbf{K} is defined as follows:

$$\mathbf{L} = \mathbf{K}(:, \mathcal{A}) \mathbf{K}(\mathcal{A}, \mathcal{A})^{-1} \mathbf{K}(:, \mathcal{A})^T \quad (19)$$

The construction of \mathcal{A} crucially influences the prediction performance. Note that `mklearn` defines a method to construct \mathcal{A} .

Algorithm 1: The mklaren algorithm pseudocode.

Input:

$\{\mathbf{x}_1, \mathbf{x}_2, \dots, \mathbf{x}_n\}$ set of objects in \mathcal{X} ,
 k_1, k_2, \dots, k_p kernel functions on $\mathcal{X} \times \mathcal{X}$,
 $\mathbf{y} \in \mathbb{R}^n$ regression targets, with $\mathbf{1}^T \mathbf{y} = 0$,
 K maximum total rank,
 δ number of look-ahead columns,
 λ regularization parameter.

Result:

$\mathbf{G}_1 \in \mathbb{R}^{n \times j_1}, \mathbf{G}_2 \in \mathbb{R}^{n \times j_2}, \dots, \mathbf{G}_p \in \mathbb{R}^{n \times j_p}$,
 Cholesky factors,
 $\mathbf{H} \in \mathbb{R}^{n \times K}$ combined feature space,
 $\mathcal{A}_1, \mathcal{A}_2, \dots, \mathcal{A}_p$ active sets of pivot indices,
 $\boldsymbol{\mu} \in \mathbb{R}^n$ regression line on the training set,
 $\boldsymbol{\beta} \in \mathbb{R}^K$ regression coefficients.

```

1 Initialize:
2    $\mathbf{H} = \mathbf{0}$ ,
3   residual  $\mathbf{r} = \mathbf{y}$ ,
4   bisector  $\mathbf{u} = \mathbf{0}$ ,
5   regression line  $\boldsymbol{\mu} = \mathbf{0}$ ,
6   active sets  $\mathcal{A}_q = \emptyset$  and counters  $j_q = 0$  for  $q \in \{1, \dots, p\}$  .
7 Compute standard Cholesky Decompositions with  $\delta$  look-ahead columns for
    $\mathbf{G}_1, \mathbf{G}_2, \dots, \mathbf{G}_p$ .
8 while  $\sum_q j_q < K$  do
9   Compute  $\hat{a}_{q,i}$  and  $\hat{c}_{q,i}$  for each kernel  $q$  and pivot  $i \notin \mathcal{A}_q$  (Eq. 14)
10  Select  $q, i$  based on the minimum in Eq. 11
11  Compute  $\mathbf{g}_{q,i}$  (Eq. 2) and  $\mathbf{h}_{q,i}$  (Eq. 4)
12     $\mathbf{G}_q(:, j_q) \leftarrow \mathbf{g}_{q,i}$ 
13     $\mathbf{H}(:, \sum_q j_q) \leftarrow \mathbf{h}_{q,i}$ 
14     $j_q \leftarrow j_q + 1, \mathcal{A}_q \leftarrow \mathcal{A}_q \cup \{i\}$ 
15  Recompute  $\mathbf{G}_q(:, j_q+1:j_q+\delta)$  using standard ICD
16  Compute true  $a_{q,i}$  and  $c_{q,i}$  (Eq. 11)
17  Compute the bisector  $\mathbf{u}$  of columns in  $\mathbf{H}$  except  $h_{q,i}$  (Eq. 33)
18  Compute  $\gamma$  for  $\mathbf{h}^{(m)} = \mathbf{h}_{q,i}$  (Eq. 11) and update
19     $\boldsymbol{\mu} \leftarrow \boldsymbol{\mu} + \gamma \mathbf{u}$ 
20     $\mathbf{r} \leftarrow \mathbf{r} - \gamma \mathbf{u}$ 
21 Solve linear system  $\mathbf{H}\boldsymbol{\beta} = \boldsymbol{\mu}$  for  $\boldsymbol{\beta}$  using Eq. 18.
```

Proposition. *The Incomplete Cholesky decomposition with pivots $\mathcal{A} = \{i_1, i_2, \dots, i_j\}$ yields the same approximation as the Nyström approximation using the active set \mathcal{A} .*

$$\mathbf{L} = \mathbf{G}\mathbf{G}^T = \mathbf{K}(:, \mathcal{A})\mathbf{K}(\mathcal{A}, \mathcal{A})^{-1}\mathbf{K}(:, \mathcal{A})^T \quad (20)$$

The proof follows directly from Bach and Jordan (2005), Proposition 1. There exists an unique matrix \mathbf{L} that is: (i) *symmetric*, (ii) *has the column space spanned by $\mathbf{K}(:, \mathcal{A})$* and (iii) $\mathbf{L}(:, \mathcal{A}) = \mathbf{K}(:, \mathcal{A})$. It follows that both Incomplete Cholesky decomposition and the Nyström approximation result in the same approximation matrix \mathbf{L} .

Corollary. Let $\mathbf{G} \in \mathbb{R}^{n \times K}$ be the Cholesky factors obtained on the training set $\{\mathbf{x}_1, \mathbf{x}_2, \dots, \mathbf{x}_n\}$ using pivots indices \mathcal{A} . Let $\mathbf{K}(*, \mathcal{A})$ be the values of the kernel function $k(\mathbf{x}^*, \mathbf{x}_i)$ evaluated for all test samples \mathbf{x}^* and training samples in the active set \mathbf{x}_i , for $i \in \mathcal{A}$. The Cholesky factors $\mathbf{G}^* \in \mathbb{R}^{t \times K}$ for test samples $\{\mathbf{x}_1^*, \mathbf{x}_2^*, \dots, \mathbf{x}_t^*\}$ are inferred using the linear transform $\mathbf{T} = \mathbf{K}(\mathcal{A}, \mathcal{A})\mathbf{K}(\mathcal{A}, :)\mathbf{G}(\mathbf{G}^T\mathbf{G})^{-1}$.

$$\begin{aligned} \mathbf{G}^*\mathbf{G}^T &= \mathbf{K}(*, \mathcal{A})\mathbf{K}(\mathcal{A}, \mathcal{A})^{-1}\mathbf{K}(\mathcal{A}, :) \\ &\implies \\ \mathbf{G}^* &= \mathbf{K}(*, \mathcal{A})\mathbf{K}(\mathcal{A}, \mathcal{A})\mathbf{K}(\mathcal{A}, :)\mathbf{G}(\mathbf{G}^T\mathbf{G})^{-1} \\ &= \mathbf{K}(*, \mathcal{A})\mathbf{T} \end{aligned} \quad (21)$$

■

The matrix $\mathbf{T} \in \mathbb{R}^{K \times K}$ is inexpensive to compute and can be stored permanently after the training phase. Hence, the Cholesky factors \mathbf{G}^* are computed from the inner product between the test and the active sets $\mathbf{K}(\mathcal{A}, *)$. The combined feature matrix $\mathbf{H}^* \in \mathbb{R}^{t \times K}$ and the predictions $\boldsymbol{\mu}^* \in \mathbb{R}^t$ are obtained after centering and normalization against the training Cholesky factors \mathbf{G} :

$$\begin{aligned} \mathbf{H}^*(:, j) &= \frac{\mathbf{G}^*(:, j) - \mathbf{P}\mathbf{G}(:, j)}{\|\mathbf{P}\mathbf{G}(:, j)\|} \text{ for } j \in 1 \dots K \\ \boldsymbol{\mu}^* &= \mathbf{H}^*\boldsymbol{\beta} \end{aligned} \quad (22)$$

where $\mathbf{P} = \mathbf{I} - \frac{\mathbf{1}\mathbf{1}^T}{n}$ and $\boldsymbol{\beta}$ is defined in Eq. 18.

3.3 Computing the dual coefficients

Regardless of using the approximation to kernels, a limited form of model interpretation is still possible for a certain class of kernels. Again, we show the approach for one kernel matrix and the combined feature matrix \mathbf{H} while the computation for multiple kernels is analogous.

Kernel ridge regression is often stated in terms of dual coefficients $\boldsymbol{\alpha} \in \mathbb{R}^n$, satisfying the relation:

$$\mathbf{H}^T\boldsymbol{\alpha} = \boldsymbol{\beta} \quad (23)$$

This is an overdetermined system of equations. The vector $\boldsymbol{\alpha}$ with minimal norm can be obtained by solving the following least-norm problem:

$$\begin{aligned} & \text{minimize } \|\boldsymbol{\alpha}\|_2 \\ & \text{subject to } \mathbf{H}^T \boldsymbol{\alpha} = \boldsymbol{\beta} \end{aligned} \quad (24)$$

The problem has an analytical solution equal to

$$\boldsymbol{\alpha} = \mathbf{H}(\mathbf{H}^T \mathbf{H})^{-1} \boldsymbol{\beta} \quad (25)$$

Obtaining dual coefficients $\boldsymbol{\alpha}$ can be useful if the range of the explicit feature map induced by a kernel k is finite, such that $k(x, x') = \Phi(\mathbf{x})\Phi(\mathbf{x}')$, $\Phi : \mathcal{X} \mapsto \mathbb{R}^P$ which is the case for linear, polynomial, and various string kernels (Sonnenburg et al., 2005). An interpretation of regression coefficients in the range of Φ , $\boldsymbol{\beta}_\Phi \in \mathbb{R}^P$ is obtained by computing the matrix $\Phi \in \mathbb{R}^{n \times P}$ for the training set and considering

$$\boldsymbol{\beta}_\Phi = \Phi^T \boldsymbol{\alpha}. \quad (26)$$

Moreover, if the vector $\boldsymbol{\alpha}$ is sparse, only the relevant portions of Φ need to be computed. This condition can be enforced by using techniques such as matching pursuit when solving for $\boldsymbol{\alpha}$ (Bach et al., 2010).

3.4 ℓ_2 norm regularization

Regularization is achieved by constraining the norm of weights $\|\boldsymbol{\beta}\|$. Zou and Hastie (2005) prove the following lemma, which shows that ℓ_2 regularized regression problem can be stated as ordinary least squares using an appropriate augmentation of the data \mathbf{X}, \mathbf{y} . The following lemma assumes for all l , $\|\mathbf{X}(:, l)\| = 1$, $\mathbf{1}^T \mathbf{X}(:, l) = 0$ and $\mathbf{1}^T \mathbf{y} = 0$.

Lemma. Define the augmented data set $\mathbf{X}^\lambda, \mathbf{y}^\lambda$ to equal

$$\begin{aligned} \mathbf{X}^\lambda &= \sqrt{(1 + \lambda)} \begin{pmatrix} \mathbf{X} \\ \sqrt{\lambda} \mathbf{I} \end{pmatrix} \\ \mathbf{y}^\lambda &= \begin{pmatrix} \mathbf{y} \\ \mathbf{0} \end{pmatrix}. \end{aligned}$$

The least-squares solution of $\mathbf{X}^\lambda \boldsymbol{\beta} = \mathbf{y}^\lambda$ is then equivalent to Ridge regression of the original data \mathbf{X}, \mathbf{y} with parameter λ . For proof, see Zou and Hastie (2005). The augmented dataset can be included in LAR to achieve the ℓ_2 -regularized solution. This is achieved by modifying the columns of the combined feature matrix in Eq. 5:

$$\mathbf{h}_{q,i}^\lambda = \mathbf{P} \begin{pmatrix} \mathbf{P} \mathbf{g}_{q,i} \\ 0 \\ 0 \\ \dots \\ \lambda \\ \dots \\ 0 \end{pmatrix} / \left\| \mathbf{P} \begin{pmatrix} \mathbf{P} \mathbf{g}_{q,i} \\ 0 \\ 0 \\ \dots \\ \lambda \\ \dots \\ 0 \end{pmatrix} \right\| \quad (27)$$

This definition is now equivalent to performing LAR in augmented space \mathbf{H}^λ , resulting in an ℓ_2 regularized solution for $\boldsymbol{\mu}$ after K steps of the approximations. It is straightforward to modify Eq. 11, and Eq. 14-16 for $\mathbf{h}_{q,i}^\lambda$.

3.5 Computational complexity

The `mklearn` algorithm scales as a linear function of both the number of data points n and kernels p . The computational complexity is

$$O(n\delta^2 + K(K^2 + np\delta^2 + n\delta^2) + nK^2 + K^3) = O(K^3 + npK\delta^2). \quad (28)$$

The look-ahead Cholesky decompositions are standard Cholesky decompositions with δ pivots and complexity $O(n\delta^2)$. The main loop is executed K times. The selection of kernel and pivot pairs is based on the LAR criterion, which includes inverting $\mathbf{H}_A^T \mathbf{H}_A$ of size $K \times K$, thus having a complexity of K^3 . However, as each step is a rank-one modification to $\mathbf{H}_A^T \mathbf{H}_A$, the Morrison-Sherman-Woodbury lemma on matrix inversion (Meyer, 2000) can be used to achieve complexity $O(K^2)$ per update. The computation of correlations with the bisector in Eq. 14 and residuals are computed for p kernels in $O(np\delta^2)$. Recomputation of δ Cholesky factors requires standard Cholesky steps of complexity $O(n\delta^2)$. The computation of the gradient step is of the same complexity as the gradient step. Updating the regression line is $O(n)$. The QR decomposition in Eq. 18 takes $O(nK^2)$ and the computation of linear transform \mathbf{T} in Eq. 21 is of $O(K^3 + nK^2)$ complexity.

4. Experiments

In this section, we provide an empirical evaluation of the proposed method on known regression datasets. We compare `mklearn` with several well-known low-rank matrix approximation methods: Incomplete Cholesky Decomposition (`icd`, (Fine and Scheinberg, 2001)), Cholesky with side Information (`csi`, (Bach and Jordan, 2005)) and the Nyström method (Nyström, (Williams and Seeger, 2001)).

We also compare `mklearn` with a family of state-of-the-art multiple kernel learning methods that use the full-kernel matrix. The comparison was performed on a sentiment analysis data set with a large number of rank-one kernels (Cortes et al., 2012).

4.1 Comparison with low-rank approximations

The main advantage of `mklearn` over established kernel matrix approximation methods is simultaneous approximation of multiple kernels, which considers the current approximation to the regression line and greedily selects the next kernel and pivot to include in the decomposition. To elucidate this, we performed a comparison on eight known regression datasets: `abalone`, `bank`, `boston`, `comp-active`, `diabetes`, `ionosphere`, `kinematics`, `pumadyn`¹².

Similar to Cortes et al. (2012), seven Gaussian kernels with different length scale parameters are used. The Gaussian kernel function is defined as $k(x, y) = \exp\{-\gamma\|\mathbf{x} - \mathbf{y}\|^2\}$, where the length scale parameter γ is in range $2^{-3}, 2^{-2}, \dots, 2^0, \dots, 2^3$. For approximation methods `icd`, `csi` and Nyström, each kernel matrix was approximated independently using

¹<http://archive.ics.uci.edu/ml/>

²<http://www.cs.toronto.edu/~delve/data/datasets.html>

a fixed maximum rank K . The combined feature space of seven kernel matrices was used with ridge regression.

For **mklaren**, the approximation is defined simultaneously for all kernels and the maximum rank was set to $7K$, i.e., seven times the maximum rank of individual kernels used in **icd**, **csi** and **Nyström**. Thus, the low-rank feature space of all four methods had exactly the same dimension. The uniform kernel combination (**uniform**) using the full-kernel matrix was included as an empirical lower bound.

The performance was assessed using 5-fold cross-validation as follows. Initially up to 1000 data points were selected randomly from the dataset. For each random split of the data set, a *training set* containing 60% of the data was used for kernel matrix approximation and fitting the regression model. A *validation set* containing 20% of the data was used to select the regularization parameter λ from range $10^{-3}, 10^{-2}, \dots, 10^0, \dots, 10^3$. The final reported performance using root mean square error (RMSE) was obtained on the *test set*

Dataset	mklaren	csi	icd	Nyström	uniform
boston	4.393 \pm 0.432	4.762 \pm 0.598	6.703 \pm 0.354	6.611 \pm 1.272	3.109 \pm 0.274
kin	0.018 \pm 0.000	0.025 \pm 0.003	0.067 \pm 0.006	0.065 \pm 0.006	0.013 \pm 0.000
pumadyn	1.252 \pm 0.032	1.650 \pm 0.169	4.024 \pm 0.655	3.882 \pm 0.803	1.210 \pm 0.070
abalone	2.638 \pm 0.116	2.768 \pm 0.187	2.906 \pm 0.222	2.939 \pm 0.197	2.499 \pm 0.118
comp	5.288 \pm 0.461	7.520 \pm 1.852	14.111 \pm 1.123	13.763 \pm 0.580	0.750 \pm 0.203
ionosphere	0.283 \pm 0.017	0.310 \pm 0.022	0.380 \pm 0.010	0.377 \pm 0.015	0.292 \pm 0.025
bank	0.036 \pm 0.001	0.046 \pm 0.005	0.101 \pm 0.011	0.128 \pm 0.010	0.034 \pm 0.001
diabetes	54.680 \pm 3.61	54.953 \pm 3.018	63.715 \pm 5.970	68.117 \pm 3.947	62.142 \pm 3.991

Dataset	mklaren	csi	icd	Nyström	uniform
boston	3.792 \pm 0.454	4.481 \pm 0.689	5.499 \pm 0.680	5.677 \pm 0.609	3.109 \pm 0.274
kin	0.016 \pm 0.001	0.018 \pm 0.000	0.059 \pm 0.008	0.054 \pm 0.009	0.013 \pm 0.000
pumadyn	1.257 \pm 0.032	1.268 \pm 0.035	3.552 \pm 0.767	3.581 \pm 0.660	1.210 \pm 0.070
abalone	2.526 \pm 0.097	2.591 \pm 0.111	2.777 \pm 0.194	2.820 \pm 0.220	2.499 \pm 0.118
comp	3.100 \pm 0.942	5.318 \pm 1.298	12.646 \pm 0.548	11.288 \pm 2.365	0.750 \pm 0.203
ionosphere	0.234 \pm 0.028	0.254 \pm 0.030	0.341 \pm 0.012	0.331 \pm 0.016	0.292 \pm 0.025
bank	0.035 \pm 0.001	0.036 \pm 0.001	0.067 \pm 0.005	0.110 \pm 0.012	0.034 \pm 0.001
diabetes	55.580 \pm 3.634	55.220 \pm 3.56	58.793 \pm 5.606	60.747 \pm 2.377	62.142 \pm 3.991

Dataset	mklaren	csi	icd	Nyström	uniform
boston	3.493 \pm 0.489	4.191 \pm 0.878	4.657 \pm 0.664	5.220 \pm 0.751	3.109 \pm 0.274
kin	0.014 \pm 0.000	0.018 \pm 0.000	0.043 \pm 0.018	0.040 \pm 0.014	0.013 \pm 0.000
pumadyn	1.255 \pm 0.038	1.251 \pm 0.027	3.015 \pm 0.702	2.448 \pm 0.742	1.210 \pm 0.070
abalone	2.500 \pm 0.110	2.545 \pm 0.095	2.597 \pm 0.128	2.702 \pm 0.159	2.499 \pm 0.118
comp	1.330 \pm 0.409	4.791 \pm 2.805	9.845 \pm 2.085	9.744 \pm 2.005	0.750 \pm 0.203
ionosphere	0.221 \pm 0.012	0.228 \pm 0.018	0.304 \pm 0.024	0.266 \pm 0.033	0.292 \pm 0.025
bank	0.034 \pm 0.002	0.035 \pm 0.001	0.042 \pm 0.009	0.101 \pm 0.020	0.034 \pm 0.001
diabetes	55.628 \pm 3.597	55.214 \pm 4.03	56.608 \pm 4.488	57.560 \pm 2.425	62.142 \pm 3.991

Table 1: Comparison of regression performance (RMSE) on test sets via 5-fold cross-validation for different values of rank (K). Shown in bold is the low-rank approximation method with lowest RMSE. **Top** $K=14$. **Middle** $K=28$. **Bottom** $K=42$.

with remaining 20% of the data. All variables were standardized and the targets \mathbf{y} were centered to the mean. The look-ahead parameter δ was set to 10 for **mklaren** and **csi**.

The results for different settings of K are shown in Table 1. Not surprisingly, the performance of supervised **mklaren** and **csi** is consistently superior to unsupervised **icd** and **Nyström**. Moreover, **mklaren** outperforms **csi** on the majority of regression tasks, especially at lower values of K . At higher values of K , the difference vanishes as all approximation methods recover sufficient information of the feature space induced by the kernels.

Dataset	n	mklaren	csi	icd	Nyström
boston	506	42	63	> 140	119
kin	1000	63	> 140	> 140	> 140
pumadyn	1000	49	> 140	56	98
abalone	1000	21	28	35	49
comp	1000	49	63	> 140	> 140
ionosphere	351	14	14	42	35
bank	1000	21	42	42	112
diabetes	442	14	14	14	21

Table 2: Comparison of minimal rank for which the RMSE differs by at most one standard deviation to RMSE obtained with the full kernel matrices using uniform alignment. The number of data samples is denoted by n . Shown in bold is the method with lowest maximal rank K to achieve equivalent performance to **uniform**.

It is interesting to compare the utilization of the vectors in the low-dimensional feature space. Table 2 shows the minimal setting of K where the performance is at most one standard deviation away from the performance obtained by **uniform**. On seven out of eight datasets, **mklaren** reaches equivalent performance to **uniform** at the smallest setting of K . The differences in ranks among all four evaluated methods in Table 2 are statistically significant ($p=0.0012$, Friedman rank-sum test). Additionally, **mklaren** and **csi** difference in ranks is statistically significant (Wilcoxon signed-rank test, $p=0.03552$). On only the diabetes dataset, the unsupervised **icd** and **Nyström** outperform the supervised methods at low ranks. However, at higher setting of K the performance of **csi** and **mklaren** overtakes **icd** and **Nyström** as can be seen in Table 1.

Overall the results confirm the utility of the greedy approach to select not only pivots, but also the kernels to be approximated and suggest **mklaren** to be the method of choice when competitive performance at very low-rank feature spaces is desired. The kernels that are not added to the decomposition can be discarded. This point is discussed further in the next subsection.

4.2 Comparison with MKL methods on rank-one kernels

The comparison of **mklaren** to multiple kernel learning methods using the full kernel matrix is challenging as it is unrealistic to expect improved performance with low-rank approximation methods. Although the restriction to low-rank feature spaces may result in implicit regularization and improved performance as a consequence, the difference in implicit dimension of the feature space makes the comparison difficult (Bach, 2012).

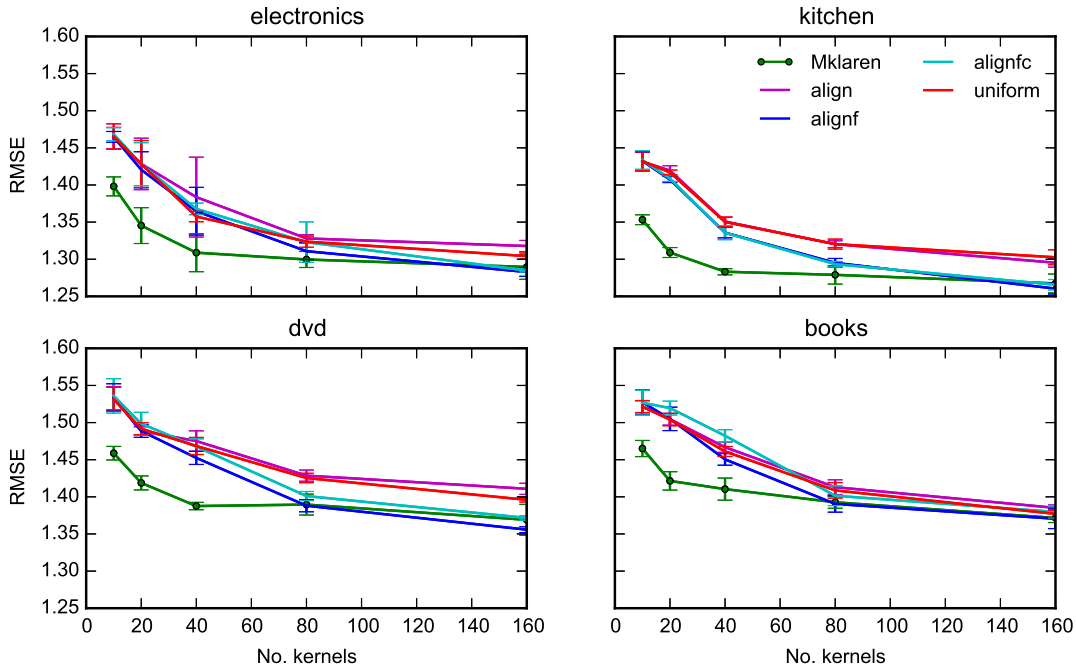


Figure 3: RMSE on the test set for MKL methods. The rank K is equal to the number of kernels included.

We focus on the ability of `mklaren` to select from a set of kernels in a way that takes into account the implicit correlations between the kernels. To this end, we built on the empirical analysis of Cortes et al. (2012). The mentioned reference used four well-known sentiment analysis datasets compiled by Blitzer et al. (2007). In each dataset, the examples are user reviews of products and the target is the product rating in a discrete range 1..5. The features are counts of 4000 most frequent unigrams and bigrams in each dataset. Each feature was represented by a rank-one kernel, thus enabling the use of multiple kernel learning for feature selection and explicit control over feature space dimension. The datasets contain moderate number of examples: books ($n = 5501$), electronics ($n = 5901$), kitchen ($n = 5149$) and dvd ($n = 5118$). The splits into *training* and *test* part were readily included as a part of the data set.

We compared `mklaren` with three state-of-the-art multiple kernel learning methods for comparison. All methods are based on maximizing centered kernel alignment Cortes et al. (2012). The `align` method infers the kernel weights independently, while `alignnf` and `alignfc` consider the between-kernel correlations when maximizing the alignment. The combined kernel learned by all three methods was used with kernel ridge regression model. The `align` method is linear in the number of kernels (p), while `alignnf` and `alignfc` are cubic as they include solving an unconstrained (`alignnf`) or a constrained (`alignfc`) QP.

When testing for different ranks K , the features were first filtered according to the descending centered alignment metric for `align`, `alignnf`, `alignfc` prior to optimization. When using `mklaren` the K pivot columns were selected from the complete set of 4000

features. The parameter δ was set to 1. Note that in this scenario, **mklaren** is equivalent to the original LAR algorithm, thus excluding the effect of low-rank approximation and comparing only the kernel selection part. This way, the same dimension of the feature space was ensured.

The performance was measured via 5-fold cross-validation. At each step, 80% of the *training* was used for kernel matrix approximation (**mklaren**) or determining kernel weights (**align**, **alignf**, **alignfc**). The remaining 20% of the training set was used for selecting regularization parameter λ from range $10^{-3}, 10^{-2}, \dots, 10^3$ and the final performance was reported on the *test* set using RMSE.

The results for different settings of K are shown in Fig. 3. For low settings of K , **mklaren** outperforms all four other MKL methods that assume full kernel-matrices. The performance of **mklaren** at $K=40$ is within one standard deviation of best performance using 160 features using any of the methods, showing that the greedy kernel and pivot selection criterion considers implicit correlations between kernels.

However, there is an important difference in computational complexity. Note that **mklaren** is linear in the number of kernels p , which presents a practical advantage over **alignf** and **alignfc**. The comparison of methods' implementation run times is shown on Fig. 4.

We compared the methods run times on a synthetic dataset with $p = 10$ Gaussian kernels differing in parameters, rank $K = 40$ and variable n . Since the methods (**align**, **alignf**, **alignfc**, **uniform**) require the computation of the whole kernel matrix, **mklaren** was significantly more efficient (up to 3 orders of magnitude with $n=4000$ samples).

The experiments with varying number of kernels were performed on the **books** dataset. The centered kernel alignment value can be computed efficiently due to the usage of rank-one linear kernels, without explicit computation of the outer product. This proves very efficient for **uniform** and **align** methods where the weights are computed independently. While the **mklaren** method is also linear in the number kernels (p), it accounts for the in-between kernel correlations. The overhead in calculating low-rank approximations is beneficiary when the number of kernels exceeds 2000. Thus, effect for accounting of between-kernel correlations is achieved at a significantly computational lower cost.

Finally, we compare the methods with respect to feature selection on the kitchen dataset. Each of the methods **mklaren**, **align**, **alignf**, and **alignfc** returns and ordering of the kernels (features). With **mklaren**, this order is obtained as the pivot columns corresponding to kernels are added to the approximation. With alignment-based methods, we use the order induced by the kernel weight vector. In Fig. 5, we display the top 40 features as obtained from each such ordering, shown as words on the horizontal axis. We incrementally add features to an *active set*. As each feature is added at step i , we infer an ordinary least-squares $\beta_{\text{OLS},i}$, which uses all features up to i . The explained variance is calculated as the ratio of the difference of the RMSE on the training set versus total variance. The arrows below each word at step i indicate the sign of the corresponding weight in $\beta_{\text{OLS},i}$.

Intuitively, the slope (change in explained variance) is higher for features corresponding to words associated to strong sentiments. This is most notable for words such as *great*, *good*, *love*, etc. Not surprisingly, the order in which features are added to the model critically influences the explained variance. Here, **mklaren** outperforms the alignment-based methods. Due to its linear complexity in the number of kernels p , the features strongly correlated to

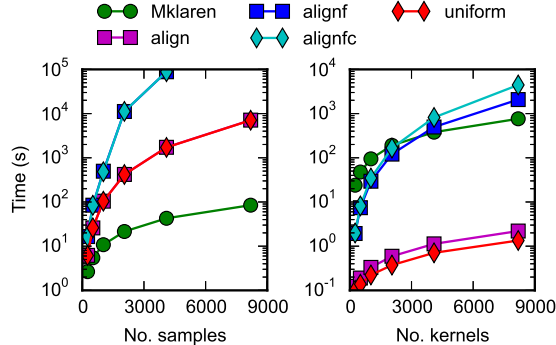


Figure 4: Comparison of running times. (left) Time versus number of samples on a synthetic dataset with $P = 10$ kernels. (right) Time versus number of kernels on **books** training dataset, $n = 4000$ samples.

the response are identified early, irrespective to their magnitude. On the other hand, the centered alignment appears to be biased towards words with a high number of nonzero entries in the dataset, such as propositions. Moreover, the word associated to negative or positive sentiments are approximately balanced, according to the signs in $\beta_{\text{OLS},i}$. The results confirm **mklaren** can be used for model interpretation.

5. Conclusion

Subquadratic complexity in the number of training examples is essential in large-scale application of kernel methods. Learning the kernel matrix efficiently from the data and the selection of relevant portions on the data early can reduce time and storage requirements further up the machine learning pipeline. The complexity with respect to the number of kernels should not be disregarded when the number of kernels is large. Using a greedy low-rank approximation to multiple kernels, we achieve linear complexity in the number of kernels and data points without sacrificing the consideration of in-between kernel correlations. Moreover, the approach learns a regression model, but is nevertheless applicable in any kernel-based model. The extension to classification or ranking tasks is an interesting subject for future work. Contrary to the recent kernel matrix approximations, we present an idea based entirely on geometric principles, which is not limited to transductive learning. With the abundance of different data representations, we expect kernel methods to remain essential in machine learning applications.

Appendix

Least-angle regression

Least-angle regression (LAR) is an *active set method*, originally designed for feature subset selection in linear regression (Friedman et al., 2001; Hesterberg et al., 2008; Efron and Hastie, 2004). A column is chosen from the set of candidates such that the correlations with the residual are equal for all active variables. This is possible because all variables (columns) are

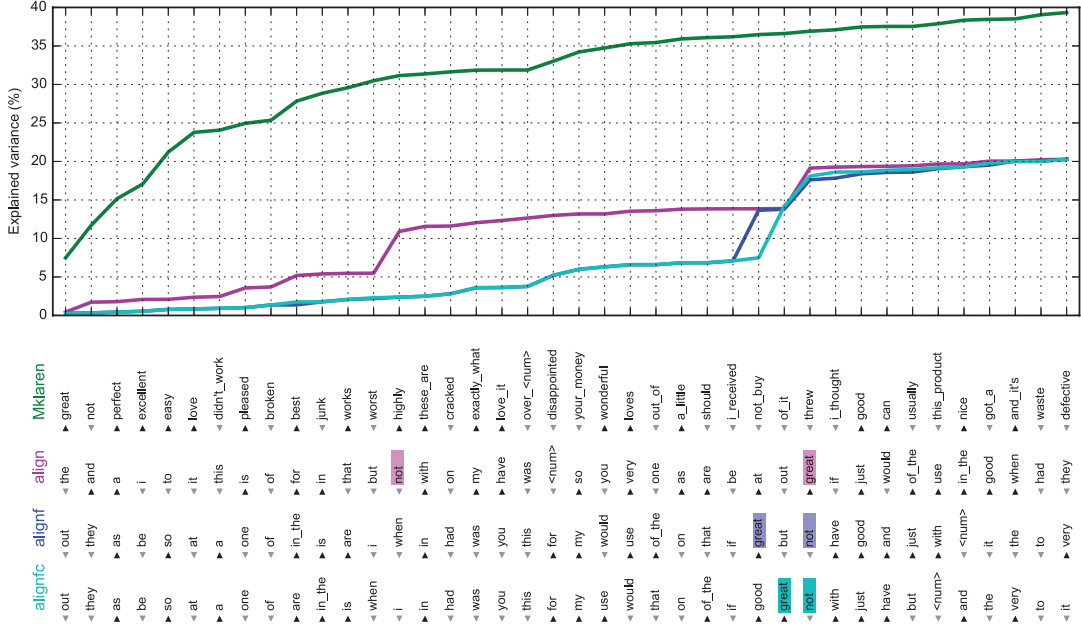


Figure 5: Increase in explained variance upon incrementally including features to an ordinary least-squares model. The order of features is determined by the magnitude of kernel weights for `align`, `alignf` and `alignfc` or the order of selection by `mklaren`. Explained variance is measured as a ratio of training RMSE vs. total variance. Arrows indicate positive (black) or negative (gray) sign of the feature in the model weight vector upon inclusion. Highlighted are words "great" and "not", which significantly alter the explained variance when discovered by `align`, `alignf` and `alignfc` models.

known *a priori*, which clearly does not hold for candidate pivot columns. The monotonically decreasing maximal correlation in the active set is therefore not guaranteed. Moreover, the addition of a column to the active set potentially affects the values in all further columns. Naively recomputing these values at each iteration would yield a computational complexity of order $O(n^2)$.

Let the predictor variables $\mathbf{x}_1, \mathbf{x}_2, \dots, \mathbf{x}_p$ be vectors in \mathbb{R}^n , arranged in a matrix $\mathbf{X} \in \mathbb{R}^{n \times p}$. The associated response vector is $\mathbf{y} \in \mathbb{R}^n$. The LAR method iteratively selects the predictor variables \mathbf{x}_j and the corresponding coefficients β_j are updated at the same time as they are moved towards their least-squares coefficients. At last step, the method reaches the least-squares solution $\mathbf{X}\beta = \mathbf{y}$.

The high-level pseudo code is as follows:

1. Start with the residual $\mathbf{r} = \mathbf{y} - \bar{\mathbf{y}}$, and regression coefficients $\beta_1, \beta_2, \dots, \beta_p = 0$.
2. Find the variable \mathbf{x}_j most correlated with \mathbf{r} .
3. Move β_j towards its least-squares coefficient until another \mathbf{x}_k has as much correlation with \mathbf{r} .

4. Move β_j and β_k in the direction towards their joint least-sq. coeff., until some new \mathbf{x}_l has as much correlation with \mathbf{r} .
5. Repeat until all variables have been entered, reaching the least-sq. solution.

Note that the method is easily modified to include early stopping, after a maximum number of selected predictor variables are included. Importantly, the method can be viewed as a version of supervised Incomplete Cholesky Decomposition of the *linear kernel* $\mathbf{K} = \mathbf{X}\mathbf{X}^T$ which corresponds to the usual inner product in \mathbb{R}^p .

Assume that the predictor variables are standardized and response has had its mean subtracted off:

$$\begin{aligned} \mathbf{1}^T \mathbf{x}_j &= 0 \text{ and } \|\mathbf{x}_j\|_2 = 1 \text{ for } j = 1, 2, \dots, p. \\ \mathbf{1}^T \mathbf{y} &= 0 \end{aligned} \tag{29}$$

Initialize the *regression line* $\boldsymbol{\mu}$, the *residual* \mathbf{r} and the *active set* \mathcal{A} :

$$\boldsymbol{\mu} = \mathbf{0}, \mathbf{r} = \mathbf{y} \text{ and } \mathcal{A} = \emptyset. \tag{30}$$

The LAR algorithm estimates $\boldsymbol{\mu} = \mathbf{X}\boldsymbol{\beta}$ in successive steps. Say the predictor \mathbf{x}_i has the largest correlation with \mathbf{r} . Then, the index i is added to the active set \mathcal{A} and the regression line and residual are updated:

$$\begin{aligned} \boldsymbol{\mu}^{\text{new}} &= \boldsymbol{\mu} + \gamma \mathbf{x}_i \\ \mathbf{r}^{\text{new}} &= \mathbf{r} - \gamma \mathbf{x}_i \end{aligned} \tag{31}$$

The step size γ is set such that a new predictor \mathbf{x}_j will enter the model after $\boldsymbol{\mu}$ is updated and all predictors in the active set as well as \mathbf{x}_j will be equally correlated to \mathbf{r} . The key parts are the selection of predictors added to the model and the calculation of the step size.

The active matrix for a subset of indices j with sign s_j is defined as

$$\begin{aligned} \mathbf{X}_A &= (\cdots s_j \mathbf{x}_j \cdots) \text{ for } j \in \mathcal{A} \\ s_j &= \text{sign}\{\mathbf{x}_j^T \mathbf{r}\} \end{aligned} \tag{32}$$

By elementary linear algebra, there exist a *bisector* \mathbf{u}_A - an equiangular vector, having $\|\mathbf{u}_A\|_2 = 1$ and making equal angles, less than 90 degrees, with vectors in \mathbf{X}_A . Define the following quantities respectively: \mathbf{X}_A the active matrix, A the normalization scalar, \mathbf{u}_A the bisector, and $\boldsymbol{\omega}$ the vector making equal angles with the columns of \mathbf{X}_A . The bisector is obtained as follows.

$$\begin{aligned} \mathbf{T}_A &= \mathbf{X}_A^T \mathbf{X}_A \\ A &= (\mathbf{1}_A^T \mathbf{T}_A \mathbf{1}_A)^{-1/2} \\ \boldsymbol{\omega} &= A \mathbf{T}_A^{-1} \mathbf{1}_A \\ \mathbf{u}_A &= \mathbf{X}_A \boldsymbol{\omega}_A \end{aligned} \tag{33}$$

The calculation of step size γ proceeds as follows. Get the maximum vector of correlations. Active set contains variables with highest absolute correlations.

$$\begin{aligned} c_j &= \mathbf{x}_j^T \mathbf{r} \\ C &= \max_j \{c_j\} \\ \mathbf{a} &= \mathbf{X}_A^T \mathbf{u}_A \end{aligned} \tag{34}$$

$$\gamma = \min_{j \in \mathcal{A}^c}^+ \left\{ \frac{C - c_j}{A_A - a_j}, \frac{C + c_j}{A_A + a_j} \right\}$$

where \min^+ is the minimum over positive components.

By Eq. 31, we the change in correlations within the active set can be expressed.

$$c_j^{\text{new}} = \mathbf{x}_j^T (\mathbf{y} - \mathbf{r}^{\text{new}}) = c_j - \gamma a_j \tag{35}$$

For the predictors in active set, we have

$$|c_j^{\text{new}}| = C - \gamma A, \text{ for } j \in \mathcal{A}. \tag{36}$$

A variable is selected from the remaining variables in \mathcal{A}^c , such that c_j^{new} is maximal. Equating Eq. 35 and Eq. 36, and maximizing yields $\gamma = \frac{C - c_j}{A - a_j}$. Similarly, $-c_j^{\text{new}}$ for the reverse covariate is maximal at $\gamma = \frac{C + c_j}{A + a_j}$. Hence, γ is chosen in Eq. 34 as a minimal value for which an variable joins the active set.

References

- Francis Bach. Sharp analysis of low-rank kernel matrix approximations. *arXiv:1208.2015*, August 2012.
- Francis Bach, Julien Mairal, Jean Ponce, and Guillermo Sapiro. Sparse coding and dictionary learning for image analysis. In *Proceedings of IEEE International Conference on Computer Vision and Pattern Recognition*, 2010.
- Francis R. Bach and Michael I. Jordan. Predictive low-rank decomposition for kernel methods, 2005.
- Arnab Bhattacharyya and Abhishek Bhowmick. Pivoted Cholesky decomposition by Cross Approximation for efficient solution of kernel systems. *arXiv preprint arXiv:1505.06195*, pages 1–19, May 2015.
- Christopher M Bishop. *Pattern Recognition and Machine Learning*. Information Science and Statistics. Springer, 2006. ISBN 9780387310732.
- John Blitzer, Mark Dredze, and Fernando Pereira. Biographies, bollywood, boom-boxes and blenders: Domain adaptation for sentiment classification. In *ACL*, volume 7, pages 440–447, 2007.

- Yanshuai Cao, Marcus Brubaker, David Fleet, and Aaron Hertzmann. Efficient Optimization for Sparse Gaussian Process Regression. *IEEE Transactions on Pattern Analysis & Machine Intelligence*, pages 1–1, 2015. ISSN 0162-8828. doi: 10.1109/TPAMI.2015.2424873.
- Corinna Cortes, Mehryar Mohri, and Afshin Rostamizadeh. Two-stage learning kernel algorithms. In *Proceedings of the 27th International Conference on Machine Learning*, pages 239–246, 2010.
- Corinna Cortes, Mehryar Mohri, and Afshin Rostamizadeh. Algorithms for Learning Kernels Based on Centered Alignment. *Journal of Machine Learning Research*, 13:795–828, March 2012.
- Bradley Efron and Trevor Hastie. Least angle regression. *The Annals of statistics*, 32(2):407–499, 2004.
- Shai Fine and Katya Scheinberg. Efficient SVM Training Using Low-Rank Kernel Representations. *Journal of Machine Learning Research*, 2:243–264, 2001.
- Jerome Friedman, Trevor Hastie, and Robert Tibshirani. *The elements of statistical learning*, volume 1. Springer series in statistics Springer, Berlin, 2001.
- Yarin Gal and R Turner. Improving the Gaussian process sparse spectrum approximation by representing uncertainty in frequency inputs. In *Proceedings of the 32nd International Conference on Machine Learning*, 2015.
- Alex Gittens and Michael W. Mahoney. Revisiting the Nystrom Method for Improved Large-Scale Machine Learning. *arXiv preprint arXiv:1303.1849*, page 60, March 2013.
- Gene H Golub and Charles F Van Loan. *Matrix computations*, volume 3. JHU Press, 2012.
- Mehmet Gönen and Ethem Alpaydin. Supervised learning of local projection kernels. *Neurocomputing*, 73(10-12):1694–1703, June 2010. ISSN 09252312. doi: 10.1016/j.neucom.2009.11.043.
- Mehmet Gönen and Ethem Alpaydin. Multiple kernel learning algorithms. *The Journal of Machine Learning Research*, 12:2211–2268, 2011.
- Tim Hesterberg, Nam Hee Choi, Lukas Meier, and Chris Fraley. Least angle and ℓ_1 penalized regression: A review. *Statistics Surveys*, 2:61–93, 2008. ISSN 1935-7516. doi: 10.1214/08-SS035.
- J Kandola, J Shawe-Taylor, and N Cristianini. Optimizing Kernel Alignment over Combination of Kernels, 2002.
- Samuel Kaski and Mehmet Gonen. Kernelized Bayesian matrix factorization. *IEEE Transactions on Pattern Analysis & Machine Intelligence*, 36(10):2047–2060, 2014.
- Brian Kulis, MA Sustik, and IS Dhillon. Low-rank kernel learning with Bregman matrix divergences. *The Journal of Machine Learning Research*, 10:341–376, 2009.

- GRG Lanckriet and N Cristianini. Learning the kernel matrix with semidefinite programming. *Journal of Machine Learning Research*, 5:27–72, 2004.
- Quoc Le, T Sarlós, and Alex Smola. Fastfood—approximating kernel expansions in loglinear time. *Proceedings of the 30th International Conference on Machine Learning*, 28, 2013.
- Mu Li, Wei Bi, James T Kwok, and Bao-Liang Lu. Large-Scale Nyström Kernel Matrix Approximation Using Randomized SVD. *IEEE Transactions on Neural Networks and Learning Systems*, 26(1):152–164, 2015.
- Carl D Meyer. *Matrix analysis and applied linear algebra*. Siam, 2000.
- Yalda Mohsenzadeh, Hamid Sheikhzadeh, and Senior Member. Gaussian Kernel Width Optimization for Sparse Bayesian Learning. *IEEE Transactions on Neural Networks and Learning Systems*, 26(4):709–719, 2015.
- Jeffrey Pennington and Felix X Yu. Spherical Random Features for Polynomial Kernels. In *Advances in Neural Information Processing Systems*, pages 1837–1845, 2015.
- J Quiñero Candela and CE Rasmussen. A unifying view of sparse approximate Gaussian process regression. *The Journal of Machine Learning Research*, 6:1939–1959, 2005.
- Ali Rahimi and Ben Recht. Random features for large-scale kernel machines. In *Advances in Neural Information Processing Systems*, pages 1177–1184, 2007.
- Alain Rakotomamonjy and Sukalpa Chanda. ℓ_p -Norm Multiple Kernel Learning With Low-Rank Kernels. *Neurocomputing*, 143:68–79, November 2014. ISSN 09252312. doi: 10.1016/j.neucom.2014.06.019.
- Alessandro Rudi, Raffaello Camoriano, and Lorenzo Rosasco. Less is More: Nystrom Computational Regularization. *arXiv preprint arXiv:1507.04717*, 2015.
- Bernhard Schölkopf and Alexander J Smola. *Learning with kernels: Support vector machines, regularization, optimization, and beyond*. MIT press, 2002.
- Si Si, Cho-Jui Hsieh, and Inderjit Dhillon. Memory Efficient Kernel Approximation. *Proceedings of The 31st International Conference on Machine Learning*, 32, 2014.
- Edward Snelson and Zoubin Ghahramani. Sparse Gaussian processes using pseudo-inputs. In *Proceedings of the 23rd international conference on Machine learning - ICML '06*, 2006.
- Sören Sonnenburg, Gunnar Rätsch, and Bernhard Schölkopf. Large scale genomic sequence SVM classifiers. In *Proceedings of the 22nd international conference on Machine learning*, pages 848–855. ACM, 2005.
- Zoltan Szabo. Optimal rates for Random Fourier Features. In *Advances in Neural Information Processing Systems*, pages 1144–1152, May 2015.

- Andrea Vedaldi and Andrew Zisserman. Efficient additive kernels via explicit feature maps. *IEEE Transactions on Pattern Analysis & Machine Intelligence*, 34(3):480–92, March 2012. ISSN 1939-3539. doi: 10.1109/TPAMI.2011.153.
- Christopher Williams and Matthias Seeger. Using the Nyström method to speed up kernel machines. In *Proceedings of the 14th Annual Conference on Neural Information Processing Systems*, pages 682–688, 2001.
- Andrew Gordon Wilson. Kernel Interpolation for Scalable Structured Gaussian Processes (KISS-GP). *arXiv preprint arXiv:1503.01057*, 37, 2015.
- Andrew Gordon Wilson and Ryan Adams. Gaussian process kernels for pattern discovery and extrapolation. *arXiv preprint arXiv:1302.4245*, 28, 2013.
- Zenglin Xu, Rong Jin, Bin Shen, and Shenghuo Zhu. Nystrom Approximation for Sparse Kernel Methods: Theoretical Analysis and Empirical Evaluation. In *Twenty-Ninth AAAI Conference on Artificial Intelligence*, pages 3115–3121, 2015.
- Zichao Yang, Alexander J. Smola, Le Song, and Andrew Gordon Wilson. A la Carte - Learning Fast Kernels. *arXiv preprint arXiv:1412.6493*, December 2014.
- Kai Zhang, Zhuang Wang, and Fabian Moerchen. Scaling up Kernel SVM on Limited Resources : A Low-rank Linearization Approach. In *International Conference on Artificial Intelligence and Statistics*, volume XX, pages 1425–1434, 2012.
- Hui Zou and Trevor Hastie. Regularization and variable selection via the elastic net. *Journal of the Royal Statistical Society: Series B (Statistical Methodology)*, 67(2):301–320, April 2005. ISSN 1369-7412. doi: 10.1111/j.1467-9868.2005.00503.x.